

Mirror descent of Hopfield model

Hyungjoon Soh¹, Dongyeob Kim², Juno Hwang¹, Junghyo Jo^{1, 2, 3, 4, *}

¹Department of Physics Education, Seoul National University, Seoul 08826, Korea.

²Department of Physics and Astronomy, Seoul National University, Seoul 08826, Korea.

³Center for Theoretical Physics and Artificial Intelligence Institute, Seoul National University, Seoul 08826, Korea.

⁴School of Computational Sciences, Korea Institute for Advanced Study, Seoul 02455, Korea.

*Corresponding author: jojunghyo@snu.ac.kr.

Keywords: Gradient descent, exponential family, Boltzmann machine, duality

Abstract

Mirror descent is a gradient descent method that uses a dual space of parametric models. The great idea has been developed in convex optimization, but not yet widely applied in machine learning. In this study, we provide a possible way that the mirror descent can help data-driven parameter initialization of neural networks. We adopt the Hopfield model as a prototype of neural networks, we demonstrate that the mirror descent can train the model more effectively than the usual gradient descent with random parameter initialization.

1 Introduction

Recent advancement of machine learning heavily relies on optimization techniques, since machine-learning tasks can be formulated as optimization problems in general. The optimization of convex functions is a well-established subject (Nesterov et al., 2018; Wright et al., 1999). The wisdom of convex optimization is expected to contribute to solve machine-learning problems. In this study, we introduce an interesting gradient descent method, *mirror descent*, developed in the convex optimization field, and show how the mirror descent can be used for data-driven parameter initialization of machine learning.

Optimization problems can be formulated to find a minimum point θ^* of a designed objective function $L(\theta)$. Note that the model parameter $\theta = (\theta_1, \theta_2, \dots)$ is a vector in general. Here, if $L(\theta)$ is a convex function, iterative updates of θ ,

$$\theta_i^{t+1} = \theta_i^t - \alpha \frac{\partial L(\theta^t)}{\partial \theta_i}, \quad (1)$$

that follow the steepest direction of $L(\theta)$, guarantee to reach θ^* . The learning rate α controls the degree of updates. This is the gradient-descent (GD) method. This method has some unsatisfactory points. First, GD does not say anything about a starting position of θ^0 . Second, the learning rate is homogeneous ($\alpha_i = \alpha$) for every direction, which is not necessary. Third, the intuitive formula of Eq. (1) is not *covariant* under a transformation of θ . Suppose that we double $\theta_i \rightarrow 2\theta_i$. Then, θ_i^{t+1} and θ_i^t double, but $\partial L/\partial\theta_i$ halves.

To make the formula covariant, the natural gradient-descent (NGD) method is developed:

$$\theta_i^{t+1} = \theta_i^t - \alpha \sum_j \left[\frac{\partial^2 L(\theta^t)}{\partial\theta_i \partial\theta_j} \right]^{-1} \frac{\partial L(\theta^t)}{\partial\theta_j}, \quad (2)$$

where the Hessian matrix, or the curvature, of $L(\theta)$ is considered for more effective updates. NGD is a second-order method that requires to compute the Hessian matrix and its inverse. This additional computation is much costly for updating high-dimensional θ . For practical implementation, many smart numerical techniques, such as Broyden-Fletcher-Goldfarb-Shanno (BFGS) (Davidon, 1991), have been developed to approximate the inverse of the Hessian matrix. Furthermore, NGD has also been implemented for deep learning recently with Kronecker-factored approximate curvature (K-FAC) (Martens and Grosse, 2015).

Now we introduce the mirror descent (MD) that uses GD, but implies NGD. Let us first re-derive GD from a proximal gradient optimization:

$$\theta^{t+1} = \operatorname{argmin}_{\theta} \left(L(\theta) + \frac{1}{\alpha} \|\theta - \theta^t\|^2 \right), \quad (3)$$

which minimizes $L(\theta)$ under a constraint that θ should be proximal to current θ^t . The solution of Eq. (3) corresponds to the GD formula of Eq. (1). For the derivation, we used

the Taylor approximation of $L(\theta) \approx L(\theta^t) + \nabla_{\theta}L(\theta^t) \cdot (\theta - \theta^t)$. In the proximal gradient optimization, one may consider to replace the squared Euclidean distance, $\|\theta - \theta^t\|^2$, to a general distance, $D(\theta, \theta^t)$:

$$\theta^{t+1} = \underset{\theta}{\operatorname{argmin}} \left(L(\theta) + \frac{1}{\alpha} D(\theta, \theta^t) \right). \quad (4)$$

In particular, for a convex function of $F(\theta)$, the distance between θ and θ^t can be defined as the Bregman divergence:

$$D(\theta, \theta^t) = F(\theta) - F(\theta^t) - \nabla_{\theta}F(\theta^t) \cdot (\theta - \theta^t), \quad (5)$$

which measures the gap between $F(\theta)$ and its Taylor approximation, $F(\theta^t) + \nabla_{\theta}F(\theta^t) \cdot (\theta - \theta^t)$. The divergence $D(\theta, \theta^t)$ vanishes only at $\theta = \theta^t$. We plug Eq. (5) into Eq. (4), and obtain the following optimal condition,

$$\nabla_{\theta}L(\theta^t) + \frac{1}{\alpha} \left(\nabla_{\theta}F(\theta^{t+1}) - \nabla_{\theta}F(\theta^t) \right) = 0. \quad (6)$$

To represent this condition more readable, let us introduce a new variable, $\mu \equiv \nabla_{\theta}F$, which is conjugate to θ . Since the convex function $F(\theta)$ has distinct slopes μ for every position θ , knowing μ is equivalent to knowing θ . Then, the optimal condition of Eq. (6) can be reformulated as follows,

$$\mu^{t+1} = \mu^t - \alpha \nabla_{\theta}L(\theta^t). \quad (7)$$

At first sight, this equation looks like the GD formula. However, note that the gradient $\nabla_{\theta}L$ is computed for the change of θ , not for the change of μ . It is remarkable that Eq. (7) corresponds to NGD for the update in μ space, although it looks like GD (Raskutti and Mukherjee, 2015). To explicitly explain this point, another convex

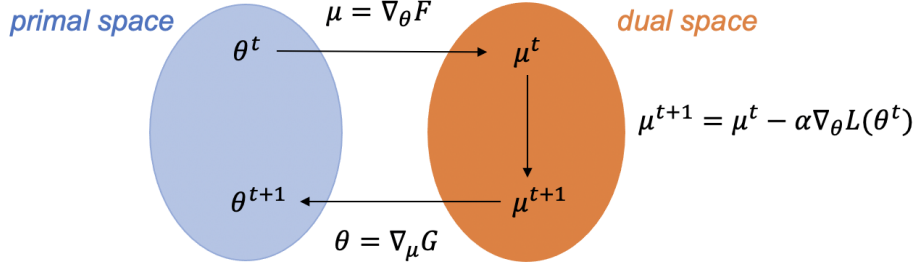


Figure 1: Mirror descent. The algorithm consists of three steps: (i) transformation from the natural parameter θ^t in primal space to μ^t in dual space; (ii) update of $\mu^t \rightarrow \mu^{t+1}$; and (iii) inverse transformation from μ^{t+1} in dual space to θ^{t+1} in primal space.

function $G(\mu)$ is introduced as a Legendre transformation of the original convex function $F(\theta)$:

$$F(\theta) + G(\mu) = \theta \cdot \mu. \quad (8)$$

The duality between θ and μ imposes $\mu = \nabla_{\theta} F$ and $\theta = \nabla_{\mu} G$. Then, we are ready to interpret $\nabla_{\theta} L$ for the change of μ using chain rules,

$$\frac{\partial L}{\partial \theta_i} = \sum_j \frac{\partial \mu_j}{\partial \theta_i} \frac{\partial L}{\partial \mu_j} = \sum_j \left[\frac{\partial^2 G}{\partial \mu_i \partial \mu_j} \right]^{-1} \frac{\partial L}{\partial \mu_j}, \quad (9)$$

where $\theta_i = \partial G / \partial \mu_i$ is used. Thus, GD-like Eq. (7) implies NGD:

$$\mu_i^{t+1} = \mu_i^t - \alpha \sum_j \left[\frac{\partial^2 G}{\partial \mu_i \partial \mu_j} \right]^{-1} \frac{\partial L(\mu^t)}{\partial \mu_j}. \quad (10)$$

Summarizing the updating procedures of MD as shown in Figure 1, (i) current θ^t in primal space is transformed to μ^t in dual space. (ii) Then, it is updated to μ^{t+1} through the first-order GD. (iii) Finally, the updated μ^{t+1} is transformed back to θ^{t+1} in primary space.

MD has a great computational merit that the first-order GD in dual space implicitly realizes the second-order NGD. However, one big obstacle for using MD is the inverse transformation to the primal space, which is usually not available. One exceptional case is using the p -norm as $F(\theta)$. This setup allows easy transformations between primal and dual spaces because the dual function $G(\mu)$ corresponds to the q -norm given $1/p + 1/q = 1$ (Gentile and Littlestone, 1999). The MD with p -norm has been nicely applied in deep learning (Azizan et al., 2021). One unsatisfactory point is that the p -norm of $F(\theta)$ is dependent just on θ , but it is not linked to data. We want to consider data-dependent distance $D(\theta, \theta')$ between models. In other words, $F(\theta)$ should be dependent on data. Our goal is implementing the nice optimization procedure of MD into a more realistic setup for machine learning problems.

2 Hopfield model

The Hopfield model can be a perfect prototype model for applying MD. The Hopfield model was developed to explain associative memories in neuroscience, and later it works as a basic model for generative models of neural networks (Hopfield, 1982). Suppose we observe a firing pattern of n neurons, $x = (x_1, x_2, \dots, x_n)$, and obtain a data of M patterns, $\{x(t)\}_{t=1}^M$, where t is not necessary to be time, but it may be a sample index. Given the M states, one can estimate the relative frequency of them as $\hat{P}(x) = 1/M \sum_t \delta(x - x(t))$. To model the empirical distribution, Hopfield proposed an exponential-family model:

$$P(x; W, b) = \frac{\exp(b \cdot x + xWx^T)}{Z}, \quad (11)$$

where $Z = \sum_x \exp(b \cdot x + xWx^T)$ is a normalization factor, called partition function in statistical mechanics. Note that x^T represents transpose of x . Here the model parameter b_i represents the bias of the i -th neuron determining its average activity, and W_{jk} represents the coupling strength between the j -th and the k -th neurons. Then, Hopfield noticed a good choice of parameter values:

$$\begin{aligned} b_i &= \mathbb{E}_{\hat{P}}[x_i], \\ W_{jk} &= \mathbb{E}_{\hat{P}}[x_j x_k], \end{aligned} \quad (12)$$

where $\mathbb{E}_{\hat{P}}[O] \equiv \sum_x O(x) \hat{P}(x)$ denotes expectation calculation. It is noted that the coupling strength W_{jk} depends on the correlation $\mathbb{E}_{\hat{P}}[x_j x_k]$ between two neurons. This is consistent with the Hebb's rule, 'fire together and wire together' (Hebb, 2005). Introducing a parameter vector $\theta \equiv \{b_1, b_2, \dots, W_{12}, \dots\}$ and an operator vector $O \equiv \{x_1, x_2, \dots, x_1 x_2, \dots\}$, we can simplify the model of Eq. (11) and the Hopfield solution of Eq. (12) as

$$P(x; \theta) = \frac{\exp(\theta \cdot O(x))}{Z}, \quad \theta_i = \mathbb{E}_{\hat{P}}[O_i]. \quad (13)$$

This Hopfield solution makes sense because the probability of a pattern x becomes large once $O(x)$ aligns with the average pattern of $\theta = \mathbb{E}_{\hat{P}}[O]$.

Indeed one can have a better solution that makes the model distribution $P(x; \theta)$ closer to the data distribution $\hat{P}(x)$ (Ackley et al., 1985). Boltzmann machine defines the distance between the two distributions using the Kullback-Leibler divergence:

$$L(\theta) = D_{KL} \left[\hat{P}(x) || P(x; \theta) \right] = \sum_x \hat{P}(x) \ln \frac{\hat{P}(x)}{P(x; \theta)}. \quad (14)$$

Given $L(\theta)$, it is straightforward to obtain its gradient:

$$\nabla_{\theta} L = \mathbb{E}_P[O] - \mathbb{E}_{\hat{P}}[O]. \quad (15)$$

Then, we can minimize the distance by using GD with $\nabla_{\theta}L$. Once the model and data expectations of $\mathbb{E}_P[O]$ and $\mathbb{E}_{\hat{P}}[O]$ are consistent, the gradient vanishes. Here we will use MD instead of this GD.

First, we start from the partition function, $Z = \sum_x \exp(\theta \cdot O(x))$. Its logarithm becomes a cumulant generating function, $F \equiv \ln Z$. One can easily obtain cumulants by differentiating F . For example, the first cumulant is obtained by

$$\nabla_{\theta}F = \sum_x O(x) \frac{\exp(\theta \cdot O)}{Z} = \mathbb{E}_P[O] = \mu. \quad (16)$$

It is the unique feature of the exponential family that the conjugate variable μ corresponds to the expectation value. Now we apply MD for the Hopfield model in the exponential family:

- (i) Transformation to dual space by computing expectation, $\mu^t = \mathbb{E}_{P(x;\theta^t)}[O]$;
- (ii) Parameter update through GD, $\mu^{t+1} = \mu^t - \alpha \nabla_{\theta}L(\theta^t)$;
- (iii) Reverse transformation to primary space, $\theta^{t+1} = \nabla_{\mu}G(\mu^{t+1})$.

Step (i) is computed by virtue of the exponential-family model. Then, step (ii) is also well defined with the gradient of Eq. (15). As always, the obstacle is in the reverse transformation of step (iii), because we do not have the explicit function $G(\mu)$, the Legendre transformation of $F(\theta)$.

We solve this problem by using the Taylor expansion of $G(\mu)$ at around $\mu = \mu^t$.

$$G(\mu) \approx G(\mu^t) + \sum_i \frac{\partial G(\mu^t)}{\partial \mu_i} (\mu_i - \mu_i^t) + \frac{1}{2} \sum_{j,k} \frac{\partial^2 G(\mu^t)}{\partial \mu_j \partial \mu_k} (\mu_j - \mu_j^t) (\mu_k - \mu_k^t). \quad (17)$$

For an infinitesimal change of $\mu^t \rightarrow \mu^{t+1}$, it is sufficient to know the local landscape of

$G(\mu)$. By differentiating $G(\mu)$ with respect to μ_i and evaluating at $\mu = \mu^{t+1}$, we have

$$\frac{\partial G(\mu^{t+1})}{\partial \mu_i} = \frac{\partial G(\mu^t)}{\partial \mu_i} + \sum_j \frac{\partial^2 G(\mu^t)}{\partial \mu_i \partial \mu_j} (\mu_j^{t+1} - \mu_j^t), \quad (18)$$

where the curvature is

$$\frac{\partial^2 G(\mu^t)}{\partial \mu_i \partial \mu_j} = \frac{\partial \theta_i}{\partial \mu_j} = \left[\frac{\partial \mu_j}{\partial \theta_i} \right]^{-1} = \left[\frac{\partial^2 F(\theta^t)}{\partial \theta_i \partial \theta_j} \right]^{-1}. \quad (19)$$

Here $\partial \mu_j / \partial \theta_i$ is nothing but the covariance matrix of operators O ,

$$\begin{aligned} \frac{\partial \mu_j}{\partial \theta_i} &= \frac{\partial}{\partial \theta_i} \sum_x O_j(x) \frac{\exp(\theta \cdot O(x))}{Z} \\ &= \mathbb{E}_P[O_i O_j] - \mathbb{E}_P[O_i] \mathbb{E}_P[O_j] = C_{ij}. \end{aligned} \quad (20)$$

Then, Eq. (18) becomes

$$\theta_i^{t+1} = \theta_i^t + \sum_j [C^{-1}]_{ij} (\mu_j^{t+1} - \mu_j^t). \quad (21)$$

This allows us to return primary space. One caveat of this process is that we need to compute the curvature or the covariance matrix. This process loses the merit of MD that implies the second-order method without explicit calculation of the curvature.

When the update step (ii) is incorporated into Eq. (21), NGD emerges as

$$\theta_i^{t+1} = \theta_i^t + \alpha \sum_j \left[\frac{\partial^2 F(\theta^t)}{\partial \theta_i \partial \theta_j} \right]^{-1} \frac{\partial L(\theta^t)}{\partial \theta_j}. \quad (22)$$

For the Hopfield model, the covariance matrix is identical to the Hessian matrix:

$$C_{ij} = \frac{\partial^2 F(\theta^t)}{\partial \theta_i \partial \theta_j} = \frac{\partial^2 L(\theta^t)}{\partial \theta_i \partial \theta_j}. \quad (23)$$

In summary, by using the Taylor expansion, we can run the MD algorithm for the Hopfield model. Furthermore, we realized that the MD update becomes identical to

NGD. Then, one may ask what MD and NGD are different. An important difference exists between the abstract θ in primary space and the observable μ in dual space. For GD or NGD, one should start from a random θ^0 due to no prior knowledge on θ . In contrast, μ^0 in dual space is different. The dual parameter of the exponential family corresponds to an expectation value $\mu = \mathbb{E}_P[O]$. Then, we are tempted to adopt the Hopfield solution as an initial value of $\mu^0 = \mathbb{E}_{\hat{P}}[O]$, since the data distribution is the most confident distribution at the moment. Note that we still do not know θ^0 that is conjugate to $\mu^0 = \mathbb{E}_{P(x;\theta^0)}[O] = \mathbb{E}_{\hat{P}}[O]$.

Starting from μ^0 in dual space looks great, but it has a fundamental problem. Since μ^0 represents the data distribution, it implies that $L(\theta^0) = D_{KL}[\hat{P}(x)||P(x;\theta^0)] = 0$ and $\nabla_{\theta}L(\theta^0) = 0$. The vanishing gradient keeps $\mu^1 = \mu^0$ from updating. This result makes a perfect sense, since the data distribution is the most confident one with no need to change. As an alternative choice of $\mu^0 = \mathbb{E}_{\hat{P}}[O]$, we consider the Hopfield solution as an initial value of θ^0 instead of μ^0 . It should not be confused that the μ^0 conjugate to this choice of $\theta^0 = \mathbb{E}_{\hat{P}}[O]$ is not $\mu^0 = \mathbb{E}_{\hat{P}}[O]$ any more, although it may be close to the value because the Hopfield solution makes $P(x;\theta^0)$ pretty close to $\hat{P}(x)$. Given the choice of data-driven θ^0 , MD can be interpreted as the NGD starting from the Hopfield solution.

3 Results

Now we examine the performance of MD applied in the Hopfield model by comparing the performance of the usual GD algorithm. To conduct this experiment, we first need to

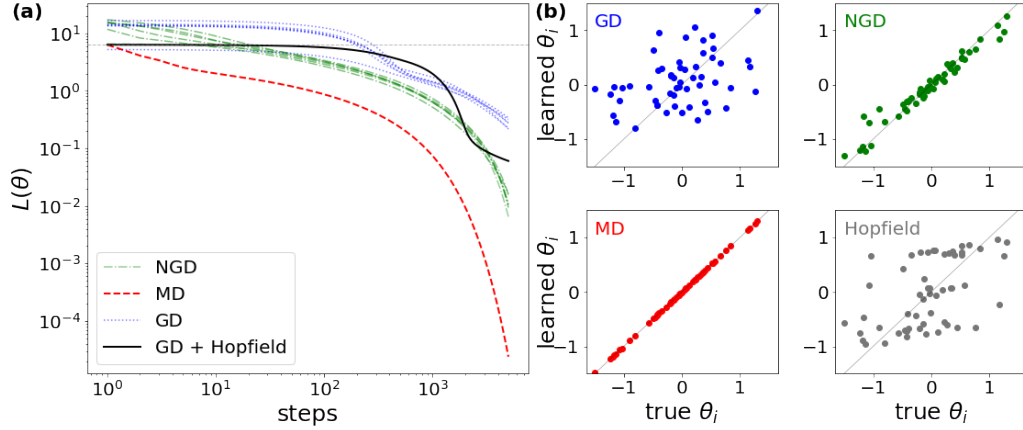


Figure 2: (a) Learning performances of different gradient methods. The Hopfield model $P(x; \theta)$ learns the data distribution $\hat{P}(x)$ of $x = (x_1, x_2, \dots, x_{10})$. The discrepancy between model and data distributions is defined as a loss $L(\theta)$. Plotted are the loss changes of (i) gradient descent (GD) with different random parameter initializations (blue dotted lines); (ii) natural gradient descent (NGD) with different random parameter initializations (green dash-single dotted lines); and (iii) GD+Hopfield, starting from the Hopfield solution (black solid line); and (iv) mirror descent (MD), starting from the Hopfield solution (red dashed line). For the simulation, a learning rate $\alpha = 0.001$ is used. (b) Accuracy of inference. The parameter of the Hopfield model is inferred from (i) GD (black); (ii) NGD (green); (iii) MD (red); and (iv) the Hopfield solution (grey). True θ_i is sampled from the standard normal distribution $\mathcal{N}(0, 1)$.

synthesize data from the Hopfield model. We obtain a true parameter set of the Hopfield model by sampling from the standard normal distribution as $\theta_i \sim \mathcal{N}(0, 1)$. Given the model parameter θ , we sampled n -dimensional binary states $x = (x_1, x_2, \dots, x_n)$ from the model distribution $P(x; \theta)$, and obtained their data distribution $\hat{P}(x)$. The goal is to infer the true θ by just using the data distribution. To circumvent the uncertainty originated from a finite size of samples, we assume that we have infinite samples. In other words, we use the ideal distribution $P(x; \theta)$ as a replacement of $\hat{P}(x)$ of infinite samples. Furthermore, for tractable integration of probability distributions over full configuration space, we confine the state dimension (e.g., $n < 20$). Without loss of generality, we used $n = 10$ for the following experiment.

We compare the convergence speed and the inference accuracy of different gradient descent methods: (i) GD; (ii) GD+Hopfield starting from the Hopfield solution; (iii) NGD; and (iv) MD. It is expected that the initial loss of MD and GD+Hopfield is lower than the loss of GD and NGD because starting from the Hopfield solution uses prior information of data unlike random initial starting. Furthermore, the second-order methods of MD and NGD lower the loss more dramatically during early iterations (Figure 2a). Note that actual computation time is not beneficial because the computation of the curvature and its inversion requires additional computation. After sufficient iterations, we examined the accuracy of inferred θ , compared with true θ , and confirmed that MD provides the most accurate inference (Figure 2b).

The inversion of covariance matrix C has no problems for a small dimension n and small values of θ . However, when n and/or θ get larger, the inversion starts to be fragile with poor inference. To make the inversion robust, we modified the covariance matrix

as $\tilde{C} = C + \epsilon I$, where I is an identity matrix. Nevertheless, NGD that starts from random initial θ^0 is still very unstable, because some eigenvalues λ of \tilde{C}^{-1} are very large to make the update of θ^{t+1} divergent. Then, we frequently observed that the loss of NGD easily diverges. The divergence of loss can be suppressed by using a smaller learning rate (i.e., inverse of the largest λ). The addition of ϵI regularizes the largest λ to be bounded to an order of $1/\epsilon$. Then, the update of θ^{t+1} stays finite for $\alpha/\epsilon < 1$. Unlike the curvature evaluated at the random initial θ^0 , the curvature at the Hopfield solution of $\theta^0 = \mathbb{E}_{\hat{P}}[O]$, shows quite robust inversion of \tilde{C} . This allows the stable update of μ^{t+1} even with a marginal learning rate (e.g., $\alpha \sim 0.1$).

MD and NGD show more effective parameter updates because they use the curvature information of the loss. The curvature is evaluated at $P(x; \theta)$ with Eq. (20) in MD. This means that the curvature should be obtained from the updated model parameters for every iteration. However, to reduce the computational cost, one may consider to use a fixed curvature C^0 evaluated at the data distribution $\hat{P}(x)$ as a proxy of updating curvatures at every step. The loss curve for these two schemes are compared in Figure 3(a). Overall, MD with updating curvatures (red dashed lines) converges faster than MD with the fixed curvature (green dotted lines). However, both MD methods outperform GD (black solid line) in spite of the 100 times smaller learning rate compared to the learning rate for GD.

Indeed the fixed curvature leads to different updating directions due to the discrepancy from the actual curvature evaluated at the updating θ^t . This ‘detouring’ takes extra steps toward a global optimum. To visualize the different learning paths on a two-dimensional space, we adopt the principle component analysis (PCA). We first

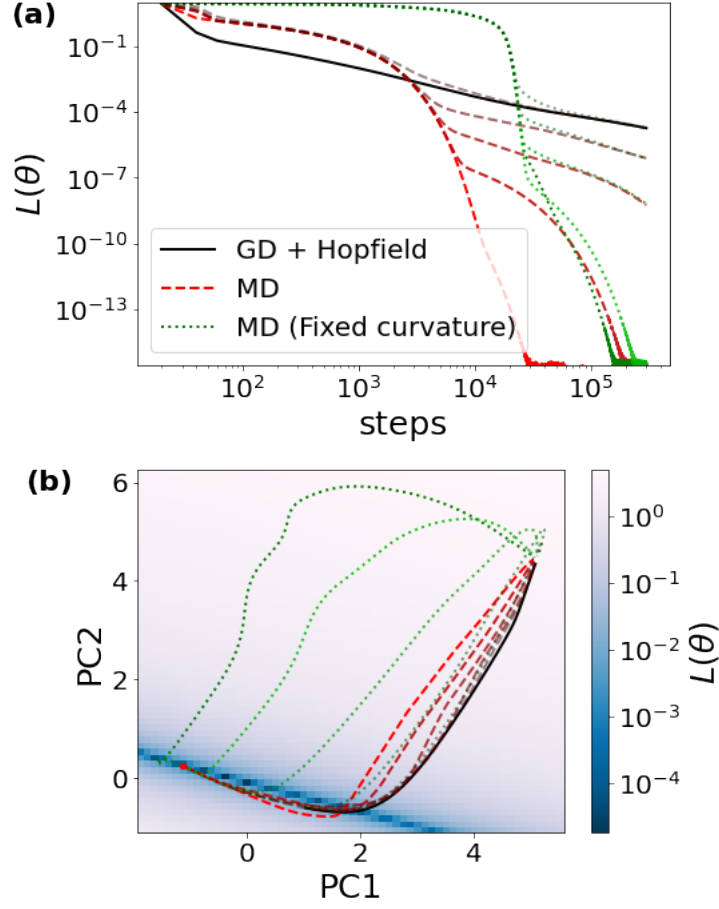


Figure 3: Mirror descent with a fixed curvature. (a) Loss curves of (i) gradient descent (GD) starting from the Hopfield solution with a learning rate $\alpha = 0.1$ (black solid line), (ii) mirror descent (MD) with updating curvatures and $\alpha = 0.001$ and $\epsilon = [10^{-6}, 10^{-5}, 10^{-4}, 10^{-3}, 10^{-2}]$ (from red to black dashed curves), and (iii) MD with a fixed curvature and $\alpha = 0.001$ and $\epsilon = [10^{-6}, 10^{-5}, 10^{-4}, 10^{-3}, 10^{-2}]$ (from green to black dotted curves). (b) Learning paths of parameters are projected on the principal component analysis (PCA) plane. Each path departs from the Hopfield solution (top right white circle), and approaches into a global optimum (bottom left red circle). True θ_i is sampled from $\mathcal{N}(0, 1.5)$.

makes a contour map of $L(\theta)$ for θ estimated at different (PC1, PC2). Then, we put the learning paths of GD, MD with updating curvatures, and MD with the fixed curvature (Figure 3(b)). Every path starts at the Hopfield solution (top right white circle), and approaches into a single global minimum (bottom left red circle) of the exponential-family model. Due to the information loss under the dimension reduction of PCA, some overshoot is observed in the learning paths on the PCA plane. We demonstrated two important points. First, MD with the fixed curvature shows a large detour to the global minimum. Nevertheless, once it approaches to the minimum, the fixed curvature becomes consistent with the curvature evaluated at the global minimum because the model distribution approaches into the data distribution. Second, increasing the regularization hyperparameter ϵ allows to approximate the curvature matrix $\tilde{C} = C + \epsilon I$ as an identity matrix. Then, MD approaches to GD. Indeed, as we increase ϵ , the learning path approaches to the path of GD.

Conclusion

In this study, we found an intriguing link between the mirror descent and the Hopfield solution. The mirror descent, a novel and beautiful formalism for natural gradient descent, has been studied in convex optimization, while it has not been widely used in machine learning. Here, we adopted the Hopfield model as a prototype of neural networks, because the conjugate parameter in dual space for such an exponential-family model corresponds to expectation values of variables in data. Thus the mirror descent using the dual space provides a possible solution for data-driven parameter initialization. The

data-driven parameter initialization is an important subject in machine learning (Seuret et al., 2017; Das et al., 2021; Chumachenko et al., 2022). We emphasize that our approach is fundamentally different from the previous popular approaches, such as He and Xavier initialization (He et al., 2015; Glorot and Bengio, 2010), that adjust initial scales of parameters depending on network size. Those approaches do not incorporate any information from data. Furthermore, the mirror descent enjoys the second-order method that considers the loss curvature of updating model parameters. In summary, the mirror descent can provide a nice optimization scheme with data-driven parameter initialization and update for training neural networks.

However, it should be noted that our study is a proof of concept. Our model is limited in various aspects, such as model structure and problems to solve. For general application of our idea to practical machine learning models such as ResNets (He et al., 2016), challenges are (i) how to incorporate hidden variables that do not appear in data; and (ii) how to generalize the idea of data-driven parameter initialization into other models beyond exponential families.

Acknowledgments

This work was supported in part by the Creative-Pioneering Researchers Program through Seoul National University, the National Research Foundation of Korea (NRF) grant (Grant No. 2022R1A2C1006871) (J. J.), and the Summer Internship Program of Artificial Intelligence Institute of Seoul National University (D. K.).

References

- Ackley, D. H., Hinton, G. E., and Sejnowski, T. J. (1985). A learning algorithm for boltzmann machines. *Cognitive science*, 9(1):147–169.
- Azizan, N., Lale, S., and Hassibi, B. (2021). Stochastic mirror descent on overparameterized nonlinear models. *IEEE Transactions on Neural Networks and Learning Systems*.
- Chumachenko, K., Iosifidis, A., and Gabbouj, M. (2022). Feedforward neural networks initialization based on discriminant learning. *Neural Networks*, 146:220–229.
- Das, D., Bhalgat, Y., and Porikli, F. (2021). Data-driven weight initialization with sylvester solvers. *arXiv preprint arXiv:2105.10335*.
- Davidon, W. C. (1991). Variable metric method for minimization. *SIAM Journal on Optimization*, 1(1):1–17.
- Gentile, C. and Littlestone, N. (1999). The robustness of the p-norm algorithms. In *Proceedings of the twelfth annual conference on Computational learning theory*, pages 1–11.
- Glorot, X. and Bengio, Y. (2010). Understanding the difficulty of training deep feedforward neural networks. *Journal of Machine Learning Research - Proceedings Track*, 9:249–256.
- He, K., Zhang, X., Ren, S., and Sun, J. (2015). Delving deep into rectifiers: Surpassing human-level performance on imagenet classification. *2015 IEEE International Conference on Computer Vision (ICCV)*, pages 1026–1034.

- He, K., Zhang, X., Ren, S., and Sun, J. (2016). Deep residual learning for image recognition. *2016 IEEE Conference on Computer Vision and Pattern Recognition (CVPR)*, pages 770–778.
- Hebb, D. O. (2005). *The organization of behavior: A neuropsychological theory*. Psychology Press.
- Hopfield, J. J. (1982). Neural networks and physical systems with emergent collective computational abilities. *Proceedings of the national academy of sciences*, 79(8):2554–2558.
- Martens, J. and Grosse, R. (2015). Optimizing neural networks with kronecker-factored approximate curvature. In *International conference on machine learning*, pages 2408–2417. PMLR.
- Nesterov, Y. et al. (2018). *Lectures on convex optimization*, volume 137. Springer.
- Raskutti, G. and Mukherjee, S. (2015). The information geometry of mirror descent. *IEEE Transactions on Information Theory*, 61(3):1451–1457.
- Seuret, M., Alberti, M., Liwicki, M., and Ingold, R. (2017). Pca-initialized deep neural networks applied to document image analysis. *2017 14th IAPR International Conference on Document Analysis and Recognition (ICDAR)*, 01:877–882.
- Wright, S., Nocedal, J., et al. (1999). Numerical optimization. *Springer Science*, 35(67-68):7.